Enhanced Knowledge in Sciences and Technology Vol. 2 No. 2 (2022) 422-431

EKST

Homepage: http://publisher.uthm.edu.my/periodicals/index.php/ekst
e-ISSN : 2773-6385

Phase Changes and Photocatalytic Activity of BIMNVOX Series for Degradation of Crystal Violet Dye in Aqueous Medium under Visible Light Irradiation

Ahlam Al–Alas[1], Niyazi A. S. Al–Areqi[1,2]*, Raya Qaid Alansi[3]

[1]Department of Chemistry, Faculty of Applied Science, Taiz Uiversity, Taiz, YEMEN.

[2]Department of Pharmacy, Faculty of Medical Sciences, Al-Saeed University, Taiz, YEMEN.

[3]Quality Assurance, Yemen Standardization, Metrology and Quality Control Organization (YSMO), Sana'a, YEMEN.

*Corresponding Author Designation

DOI: https://doi.org/10.30880/ekst.2022.02.02.045
Received 1 January 2022; Accepted 30 September 2022; Available online 23 November 2022

Abstract: A layered Aurivillius–perovskite type BIMNVOX compound with a general formula, $Bi_2Mn_x^{(IV)}V_{1-x}O_{5.5-(x/2)}$was developed as an effective photocatalyst for degradation of organic dyes. A series of BIMNVOX.*x* catalysts in the composition range $0 \leq x \leq 0.20$ were successfully prepared using the standard solid– state reaction and characterized using X–ray diffraction (XRD), differential thermal analysis (DTA), UV–vis spectrophotmetry and adsorption measurements. Then, the photocatalytic activities of synthesized catalysts were investigated for the first time through the photodegradation of crystal violet, CV dye in aqueous solution under visible light irradiation. Adsorption efficiency and photocatalytic activity of BIMNVOX.*x* catalysts were correlated well with the variation in phase crystal structures stabilized at room temperature as a function of composition. The stabilized β–BIMNVOX phase in the orthorhombic crystal system, space group *Acam* exhibited the best photocatalytic performance, though broadening band– gap energy. This can be attributed to their higher specific surface area, higher oxygen –vacancy concentration in the perovskite vanadate layers. In addition, the possible photocatalytic degradation mechanism of aqueous CV dye was clearly proposed.

Keywords: Photocatalyst, BIMNVOX, Perovskite Vanadate Layers, Crystal Violet, Oxygen Vacancies

1. Introduction

*Corresponding author: niyazi75.alareqi@gmail.com

Dyes released with industrial wastewater are of a great environmental concern. Organic dyes are widely used in many industrial and domestic processes, leading to esthetic pollution, eutrophication, and perturbations in aquatic life [1,2]. Crystal violet (CV) is a member the triphenylmethane family of dyes that has many industrial and biological applications. This large family of dyes is used widely in a variety of industrial applications, but many of them are proven to exhibit carcinogenic and mutagenic properties [3,4]. Advanced oxidation processes (AOPs) have been intensively investigated for the photodegradation of dyes in industrial wastewaters. Semiconductor- based photocatalysis has been proven to be potentially advantageous, as it costs less money and does not cause secondary contamination [5]. Among these semiconductors, TiO_2 has been widely studied for photocatalytic applications because of its thermal stability, facile preparation, cheapness and the low toxicity [6]. However, because of its relatively high band–gap, TiO_2 (3.2 eV) is only activated under ultraviolet light irradiation with wavelengths shorter than 387 nm [7,8]. This leads to severely limits the commercial applications of TiO_2 in wastewater treatments. Therefore, many researches have been made to find, design and optimize efficient photocatalysts with maximum absorption thresholds (minimum band gaps) that effectively accelerate the photocataltyic degradation of organic dyes under visible light irradiation.

Recently, the layered Aurivillius perovskite- type $Bi_4V_2O_{11}$ compound and its metal– doped analogues, acronymized as BIMEVOX.*x* ($Bi_2Me_x^lV_{1-x}O_{5.5-(5-l)x/2}$) have attracted considerable attention due to their important properties, such as in peculiar polymorphic structure and stability [9-11], very low conductivity below 300 ^oC [12], reasonable scale– electronic and ferroelectric contribution at low dopant concentrations [13,14], and noticeably narrow band gap with a potential photocatalytic efficiency under visible light irradiation[15,16].

Although, some doped members of BIMEVOX materials, such as BIALVOX and BIGAVOX reported by [15] and the BINIVOX earlier by Al-Areqi [16] have shown enhanced photocatalytic efficiency for degredation of some azo dyes within the visible spectral range as a consequence of band gap narrowing of the doped photocatalysts, there are no clear, convincing evidences to realize the actual relationship between the phase stability and photocatalytic efficiency of BIMEVOX catalysts. So in this paper, we report another new member of the BIMEVOX family, named BIMNVOX.*x*, $Bi_2Mn_x^{(IV)}V_{1-x}O_{5.5-(x/2)}$ used for the photocatalytic degradation of crystal violet dye. This study was devoted to carefully investigate the influence of metal doping on phase stability and photocatalytic properties of the BIMNVOX.*x* catalyst under visible light irradiation.

2. Materials and Methods

2.1. Catalyst preparation

A series of BIMNVOX.*x* compound of the general formula, $Bi_2Mn_x^{(IV)}V_{1-x}O_{5.5-(x/2)}$ in the composition range $0.0 \leq x \leq 0.20$, was ptrpared using the standard solid–state synthesis. Appropriate amounts of Bi_2O_3 (Aldrich, 99.9%), V_2O_5 (ABCR, 99.5%), MnO_2 (Aldrich, 99.5%) were ground together as a (1:1) acetone–toluene paste, according to the reaction equation:

$$Bi_2O_3 \quad + \frac{(1-x)}{2} \quad V_2O_5 \quad + x \quad MnO_2 \rightarrow \quad Bi_2Mn_x^{(IV)}V_{1-x}O_{5.5-(x/2)} \qquad \textbf{Eq.1}$$

The resulting paste was calcined at 650 ^oC for 20 hours. The powder was then gradually quenched in air to room temperature. The same procedure was repeated many times with an intermediate grinding in acetone– toluene solvent to ensure the completion of reaction.

2.2. Photocatalyst characterization

The X–ray diffraction (XRD) patterns were recorded on a Philips PW 1050/30 X–ray diffractometer using a CuK_α radiation (λ=1.54060 Å). The diffraction beams were collected using the Bragg– Brentano geometry in the range of $10^o \leq 2\,\theta \leq 90^o$ with an increment of 0.15^o at scantime of 1.3 sec/increment. The unit cell parameters were refined using a *POWDERX* software program. The average crystallite size was obtained from the diffraction line broadening using Scherrer equation:

$$D = \frac{0.89\lambda}{B\cos\theta} \qquad \textbf{Eq.2}$$

where D is the crystal size in nm, λ is the CuK_α radiation wavelength (λ=1.54060Å), B is the half–width of the peak in radians and θ is the corresponding diffraction angle.

Differential thermal analysis (DTA) thermograms wre collected using a Perkin–Elmer thermal analyzer. Nearly weighed 20–mg dry BIMNVOX samples were placed in α–alumina cell and experiments were then run in N_2 atmosphere. The flow rate of N_2 was maintained at 30 ml min^{-1} with a heating rate of 10 $^oC\ min^{-1}$ from ambient to 1000 ^oC.

The values of optical band–gap energy (E_g) for a series of BIMNVOX.*x* compound were estimated from UV–vis absorption spectra, recorded on a Shimadzu Scan UV–vis spectrophotometer (UV–2450) at room temperature in the wavelength range 200–800 nm. The direct band– gap energy was computed from the wavelength corresponding to the edge absorption (λ_g) using **Eq. 3** [17]:

$$E_g(eV) = \frac{1240}{\lambda_g(nm)} \qquad \textbf{Eq.3}$$

Specific surface area measurements were carried out by nitrogen adsorption– desorption isotherm at 77 K, using an Autosorb–1(Quantachrome) adsorption apparatus. The adsorption data were collected in the nitrogen partial pressure (P/P_o) range of 0.01–0.99. The specific surface areas (S_{BET}) was calculated and expressed in m^2/g, using a Brunauer–Emmett–Teller method.

2.3. Photocatalytic activity measurements

250–ml aqueous 5×10^{-4} M CV solution wsa adjusted at pH ~10.0 with a dilute aqueous solutions of NH_3 and H_2SO_4, and then placed in a photoreactor (450 ml – capacity) equipped with a magnetic stirrer. A 200–mg powdered sample of the BIMNVOX.*x* photocatayst was added into the dye aqueous solution. The resulting solution was then throughly stirred in the dark place for 25 min to reach the adsorption–desorption equilibrium. The solution was irradiated by the visible light with wavelengths greater than 400 nm using a 300–W Xe lamp located perpendicularly to the surface of solution at a constant distance of 25 cm from the surface of dye solution. Approximately 5 ml– aliquot of the reaction mixture was transferred from the photoreactor at specific time intervals (10 min) and filtered to separate the catalyst residues. The concentrations of dye against irradiation time were determined by measuring the absorbance at maximum wavelength (λ_{max}= 590 nm) using a Shimadzu UV–vis spectrophotometer (UV–2450). The photocatalytic activity of the BIMNVOX.*x* series for the photocatalytic degradation of CV dye was investigated applying a pseudo first– order kinetic model.

$$ln(C_t/C_o) = -k_{app}\ t \qquad \textbf{Eq.4}$$

where C_o and C_t are the initial concentration and remaing concentration at time, t of CV solution, respectively and k_{app} represents the apparent first– order rate constant.

3. Results and Discussion

3.1. X–ray crystallography

The XRD patterns of as–synthesized BIMNVOX.*x* series are presented in **Figure 1**. The diffraction profiles of the catalyst compositions $x < 0.10$ seem to be identical to the diffraction profile of the characteristic α–phase observed for $Bi_4V_2O_{11}$, indicating no remarkable phase change occurs in the substituted BIMNVOX.*x* with increasing Mn content upto $x < 0.10$. However, the existence of doublet sublattice peak (020) and (200) at $2\theta \sim 32^o$,and singlet peak (220) at $2\theta \sim 46.2^o$ are clear evidence for the stabilization of β–BIMNVOX.10 phase, which are characteristic to the orthorhombic symmetry with a space group, *Acam* [18]. However, the tetragonal γ′–BIMNVOX.13 phase of a space group, *I4/mmm* is stabilized, as evident by the appearance of a singlet sublattice peak indexed as (110) at $2\theta \sim 32^o$ [19].

Values of crystallographic refinements are listed in **Table 1**. It is clearly noticed that the substitution of Mn into the $Bi_4V_2O_{11}$ compound causes a dramatic increase in the unit cell parameters (particularly *a* and *c*), accompanied by the same trend in the overall lattice volume. Both density and particle size are slightly increased with increasing Mn dopant concentration. This trend is well agreed with the variation of lattice parameters, indicating that the Mn substitution has a positive contribution to the lattice expansion as a consequence of the incorporation of Mn(IV) dopant ions of larger ionic radius (0.67 Å) into the pentavalent vanadium sites (0.54 Å) of the perovskite vanadate layers [20]. However, the BET surface area ranges from 0.19 to 0.24 m^2/g, suggesting no a significant change occurs at the macroscopic level upon the Mn doping.

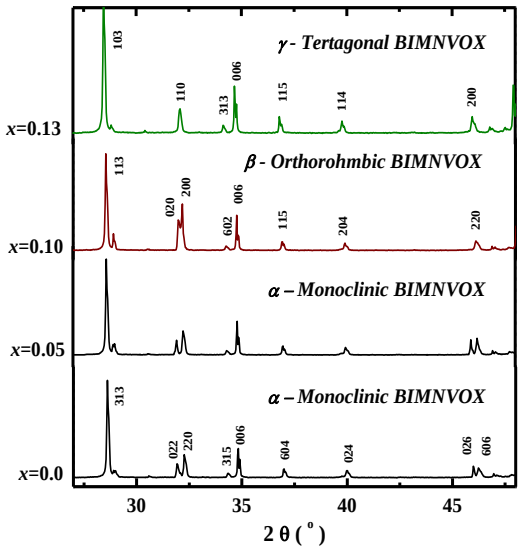

Figure 1: XRD patterns of as–prepared BIMNVOX.x series.

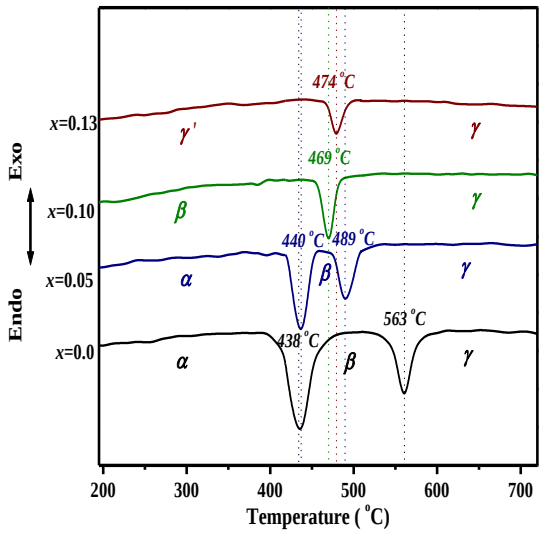

Figure2: DTA thermograms of as–prepared BIMNVOX.x series.

3.2. Thermal Analysis

Thermal stabilities and phase change temperatures of the BIMNVOX.*x* series are illustrated in the DTA thermograms (**Figure 2**). Two clear endothermic peaks are seen for the parent compound, $Bi_4V_2O_{11}$ (*x*=0) and compositions upto *x*=0.05, attributed to the successive α→β→γ transitions [21-23].

Table 1: Results of crystallographic refinements and specific surface areas of as–prepared BIMNVOX.x series

x	*Unit cell parameters*				d_{XRD} ($g\ cm^{-3}$)	*Average Crystallite size* (*μm*)	*BET surface area* (m^2/g)
	a(Å)	*b(Å)*	*c (Å)*	*V(Å³)*			
0.00	5.521	5.627	15.293	475.10	6.78	4.12	0.21
0.05	5.611	5.623	15.387	485.47	6.83	4.24	0.19
0.10	5.624	5.633	15.453	489.55	6.97	4.37	0.24
0.13	5.631	–	15.508	491.73	7.12	4.56	0.23

Also, It can be seen that the heat flow of the α→β transition is greater than that of the β→γ transition by nearly three orders of magnitude. However, the β–BIMNVOX.10 composition shows a single endothermic peak at 469 °C, attributed to the β→γ transition. While the incommensurate → commensurate, γ'→γ transition occurs for γ'–BIMNVOX.13 composition[23,24].

3.3. Optical and surface properties

UV–vis absorption spectra of three BIMNVOX.*x* compositions are shown in **Figure 3**. The parent $Bi_4V_2O_{11}$ compound displays a typical absorption in the visible region of spectrum with an absorption edge of ~ 559.08 nm, which is attributed to an intrinsic band– gap absorption of $Bi_4V_2O_{11}$ resulting from the electronic transitions occurring from *Bi6s/O2p* orbitals of the bismuthate $(Bi_2O_2)^{2+}$ layers (valence band) to the conduction band consisting of *V3d* orbitals of the $(VO_{3.5}\square_{0.5})^{2-}$ perovskite–like slabs [15,16]. It is also found that the absorption edges of the BIMNVOX.*x* series shift toward longer wavelengths as the Mn concentration increases. This trend is quite consistent with the additional contribution of *Mn3d* orbitals to the conduction band [25] and increasing oxygen vacancy concentration [22] in the perovskite vanadate layers. The effect of Mn substitution on the optical properties of the BIMNVOX.*x* system is shown in **Table 2**.

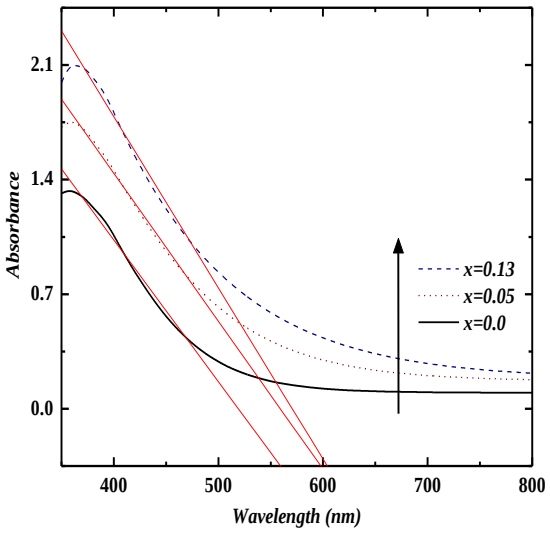

Figure3: UV–vis spectra of as- synthesized BIMNVOX.x series.

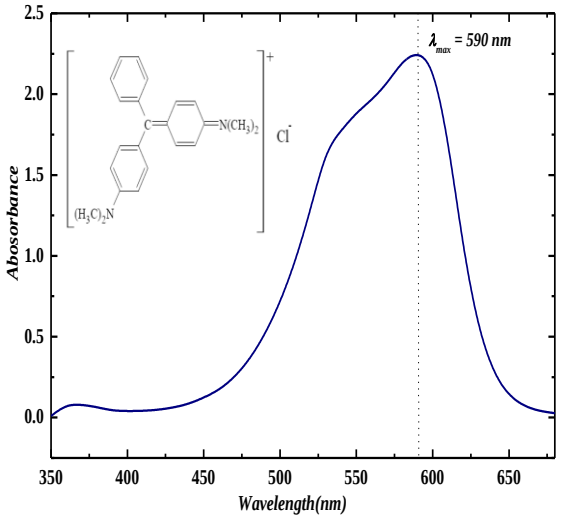

Figure 4: UV–vis spectrum of CV dye.

Table 2: Values of absortion edge wavelength and band- gap energy of BIMNVOX.*x*.

x	λ_{ab}*(nm)*	E_g *(eV)*	*SD*	*R*
0.00	559.08	2.22	0.03544	0.9925
0.05	597.91	2.07	0.02446	0.9967
0.13	604.58	2.05	0.04114	0.99457

It is clearly evident that the band–gap energy decreases with increasing Mn content, suggesting that the Mn- doping has played a positive role in the photoabsorption and photocatalytic efficiencies of $Bi_4V_2O_{11}$. The lower band–gap energy are accompanied with the otherwise increase in the corresponding special surface areas (S_{BET}) as shown in **Table 1**. This preliminary trend is basically due to the increase of active sites available on the conduction band, i.e. the negatively charged oxygen lattice positioned at the equatorial planes of perovskite vanadate layers as a result of increasing Mn substitution [26-28]. It is interesting to appoint that the CV dye molecules are expected to adsorb onto the perovskite vanadate layers and this adsorption is effectively enhanced by the coulombic interaction between negatively charged oxygen atoms of the perovskite vanadate layers (CB) of the photocatalyst and positively charged aromatic rings of CV dye molecules, suggesting that the BIMNVOX.*x* photocatalysts with layered Aurivillius– perovskite type structures can offer high specific surface areas and more active sites available for dye adsorption and consequently favorable for enhancing photocatalytic efficiency.

3.4. Photocatalytic activity and mechanism

Figure 4 shows the UV–vis spectrum of CV dye solution. The main absorbance of CV in visible region is observed at 590 nm. The photocatalytic efficiency of BIMNVOX.*x* series for photodegradation of CV dye is presented in **Figure 5**. It is also observed that the degradation rate initially shows a drastical increase with increasing Mn dopant and it is clear that the photodegradation of CV dye proceeds more rapidly when catalyzed by β– and γ′–BIMNVOX.*x* compositions.

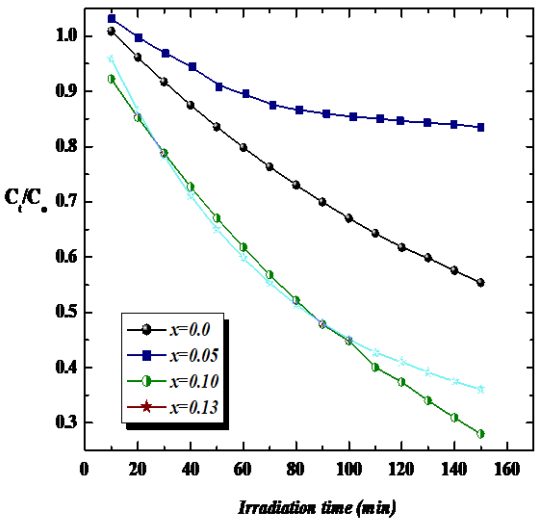

Figure 5: Photodegradation of CV dye aqueous solution catalyzed by BIMNVOX.x series under visible light irradiation.

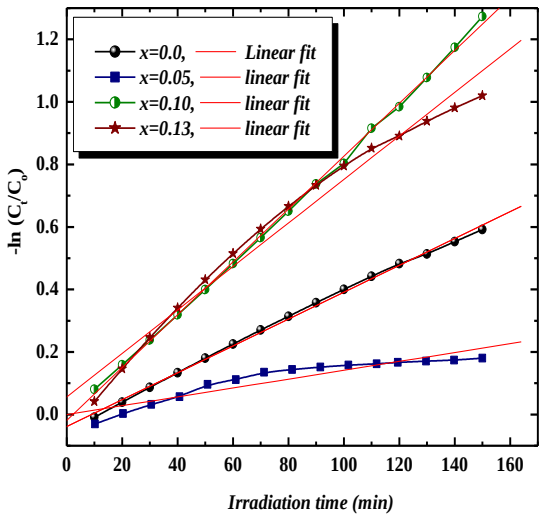

Figure 6: Linear least– squares fitting of the pseudo first–order kinetic model for the visible– light photodegradation of CV dye aqueous solution catalyzed by BIMNVOX.x series.

The values of k_{app} (min^{-1}) were computed from the slopes using the linear least– squares fitting of the first– order kinetic model as shown in **Figure 6**. The values of k_{app} as a function of the photocatalyst composition and corresponding regression determination coefficients (R^2) are listed in **Table 3**. The maximum value of k_{app} for the BIMNVOX.10 photocatalyst suggests that the photocatalytic activity of the γ'–BIMNVOX.*x* catalyst under visible light irradiation is greatly enhanced by the oxygen atoms located in the perovskite vanadate layers of BIMNVOX structure[26].

Table 3: Values of the apparent rate constant for the visible– light photodegradation of CV dye aqueous solution catalyzed by BIMNVOX.x series.

x	k_{app} $(min^{-1}) \times 10^{-3}$	*SD*	R^2
0.00	1.42	0.0091	0.93240
0.05	4.30	0.0254	0.99896
0.10	6.96	0.0499	0.95826
0.13	8.45	0.0012	0.99953

The photocatalytic degradation mechanism of CV dye using the BIMNVOX.*x* under visible light irradiation can be explained by the fact that the initial narrowing of the band gap energy of the BIMNVOX photocatalysts occurs by the Mn doping in order to enhance the visible light absorption [29]. CV molecules are then adsorbed onto the vanadate layers as a result of a coulombic interaction between negatively charged oxygen atoms of the vanadate layers and the dye molecules of positively charged conjugated chromophore. Under visible light irradiation, The proposed mechanism suggests that the adsorbed CV molecules are excited by aabsorbing visible light energy to appropriate singlet or triplet states, subsequently followed by electron ejection from the excited dye molecule onto the conduction band, while CV molecules are converted into a cationic dye radicals ($CV^{\cdot+}$) that undergoes photodegradation to yield mineralized products. The dye photocatalytic degradation reactions can be illustrated as follows [30–31]:

$$BIMNVOX + hv(Vis) \rightarrow [Bi_2O_2]_n^{2n+}(h_{VB}^+) + [V_{1-x}Mn_xO_{3.5}\square_{0.5}]_n^{2n-}(e_{CB}^-) \quad \textbf{Eq.5}$$

$$CV + hv\,(Vis) \rightarrow {}_1(CV^{\cdot+})^* \; or \; {}_3(CV^{\cdot+})^* \quad \textbf{Eq.6}$$

$$BIMNVOX + {}_1(CV^{\cdot+})^* or\ {}_3(CV^{\cdot+})^* \rightarrow CV + [V_{1-x}Mn_xO_{3.5}\square_{0.5}]_n^{2n-}(e_{CB}^-) \quad \textbf{Eq.7}$$

$$[Bi_2O_2]_n^{2n+}(h_{VB}^+) + H_2O \rightarrow BIMNVOX + H^+ + OH^- \quad \textbf{Eq.8}$$

$$[Bi_2O_2]_n^{2n+}(h_{VB}^+) + OH^- \rightarrow BIMNVOX + OH^{\cdot} \quad \textbf{Eq.9}$$

$$[V_{1-x}Mn_xO_{3.5}\square_{0.5}]_n^{2n-}(e_{CB}^-) + O_2 \rightarrow BIMNVOX + O_2^{\cdot-} \quad \textbf{Eq.10}$$

$$O_2^{\cdot-} + H^+ \rightarrow HO_2^{\cdot} \quad \textbf{Eq.11}$$

The resulting hydroxide radical ($OH^{\cdot}$) is a very strong oxidizing agent (standard redox potential +2.8 V), which can oxidize most dye molecules to mineralized products.

$${}_1(CV^{\cdot+})^* or\ {}_3(CV^{\cdot+})^* + OH^{\cdot} \rightarrow Degradation\ products \quad \textbf{Eq.12}$$

In addition the following photocatalytic degradation reactions can also occur:

$$[Bi_2O_2]_n^{2n+}(h_{VB}^+) + CV \rightarrow Oxidation\ products \quad \textbf{Eq.13}$$

$$[V_{1-x}Mn_xO_{3.5}\square_{0.5}]_n^{2n-}(e_{CB}^-) + CV \rightarrow Reduction\ products \quad \textbf{Eq.14}$$

$$Oxidation\ or\ reduction\ products + OH^{\cdot} \rightarrow Degradation\ products \quad \textbf{Eq.15}$$

4. Conclusion

In the present study, the layered Aurivillius– type oxide, *viz.* BIMNVOX.*x*, has been investigated as a photocatalyst for organic dye degradation under visible light irradiation. It has been proven that

the partial substitution of V(V) in the parent $Bi_4V_2O_{11}$ compound by Mn(IV) leads to the stabilization of photocatalytically active β– and γ′–phases exhibiting higher efficiencies for electron–hole generation and lower recombination rate of the electron–hole pair. The superior photocatalytic activity of this stabilized γ′–phase was attributed to its higher specific surface area, and higher oxygen – vacancy concentration in the perovskite vanadate layers. Accordingly, these last interesting features confer the stabilized γ′–BIMNVOX system an efficient photocatalytic activity for the degradation of organic, cationic dyes.

Acknowledgements

We would like to take the opportunity to acknowledge all those from whom I have got research and equipment facilities and have drawn all our capability to finish sthis research work:

- ***Prof. Saba Beg***, Department of Chemistry, Aligarh Muslim University, Aligarh- India for providing required chemicals and essential measurements.
- ***Prof. Kamaluddin***, Chairman, Department of Chemistry, Indian Institute of Technology (IIT)– Roorkee- India for performing DTA and Adsorption measurements.
- ***Dr. Shibum Eapen***, Scientist in Charge, Sophisticated Analytical Instrumental Facilities (SAIF)- Cochin- India for providing XRD measurements and analyses.

References

[1] G. Mckay, J.F. Porter, G.R. Prasad, The removal of dye colors from aqueous solutions by adsorption on low cost materials, *Water Air Soil Pollut.* 114 (1998) 423–438.

[2] C.C. Chen, A.J. Chaudhary, S.M. Grimes, Photodegradation of acid blue –29 and ethyl violet in the presence of NaOH and aluminum ions, *J. Hazard. Mater.* 117 (2005) 171–178.

[3] N.A. Littlefield, B.N. Blackwell, C.C. Hewitt, D.W. Gaylor, Chronic toxicity and carcinogenicity studies of gentian violet in mice, Fundam. Appl. Toxicol. 5(1985) 902–912.

[4] C-. Y. Chen a, J-.T. Kuo, H-.A. Yang, Y-.C. Chung, A coupled biological and photocatalysis pretreatment system for the removal of crystal violet from wastewater, Chemosphere 92 (2013) 695–701.

[5] N. M. Mahmoodi, M. Arami, N. Y. Limaee, Photocatalytic degradation of triazinic ring–containing azo dye (Reactive Red 198) by using immobilized TiO_2 photoreactor: Bench scale study, *J. Hazard Mater. B*133 (2006) 113–118.

[6] G. Zhang, X. Zou, J. Gonga, F. He, H. Zhang, S. Ouyang, H. Liu, Q. Zhang, Y. Liu, X. Yang, B. Hu, Characterization and photocatalytic activity of Cu-doped $K_2Nb_4O_{11}$, Journal of Molecular Catalysis A: Chemical 255 (2006) 109–116.

[7] O. Legrini, E. Oliveros, A.M. Braun, Photochemical processes for water treatment, *Chem. Rev.* 93 (1993) 671–698.

[8] I.K. Konstantinou, T.A. Albanis, TiO_2–assisted photocatalytic degradation of azo dyes in aqueous solution: kinetic and mechanistic investigations: a review, *Appl. Catal. B–Environ.* 49 (2004) 1–14.

[9] F.Abraham, M.F. Debreuille–Gresse, G. Mairesse, G. Nowogrocki, Phase transition and ionic conductivity in $Bi_4V_2O_{11}$ An oxide with a layered structure, *Solid State Ionics* 28–30(1988) 529–538.

[10] J.C. Boivin and G. Mairesse, Recent developments in fast oxide ion conductors, *Chem. Mater.* 10 (1998) 2870–2888.

[11] M. Malys, I. Abrahams, F. Krok, W. Wrobel, J.R. Dygas, The appearance of an orthorhombic BIMEVOX phase in the system $Bi_2Mg_xV_{1-x}O_{5.5-3x/2-\delta}$ at high values of x, *Solid State Ionics* 179 (2008) 82–87.

[12] S. Beg, N.A.S. Al–Areqi, Structural and electrical study of Ce^{IV}–substituted bismuth vanadate, *J. Phys. Chem. Solids* 70 (2009) 1000–1007.

[13] S. Beg, N.A.S. Al–Areqi, A. Al–Alas, Composition dependance of phase transition and ionic conductivity in BIHFVOX system, *J.Alloys.Compds.*479(2009)107–112.

[14] S. Beg, A. Al–Alas, N.A.S. Al–Areqi, Layered Aurivillius compound: Synthesis, characterization and electrical properties, *J. Alloys and Compds* 504 (2010) 413–419.

[15] V. Thakral, S. Uma, Investigation of visible light photocatalytic behavior of $Bi_4V_2O_{11-\delta}$ and BIMEVOX (ME = Al, Ga) oxides, *Mater. Res. Bull.* 45 (2010) 1250–1254.

[16] N.A.S. Al-Areqi, A. Al-Alas, Ahmed S.N. Al-Kamali, Kh.A.S. Ghaleba, Kh. Al-Mureish, Photodegradation of 4-SPPN dye catalyzed by Ni(II)-substituted $Bi_2VO_{5.5}$ system under visible light irradiation: Influence of phase stability and perovskite vanadate–oxygen vacancies of photocatalyst, Journal of Molecular Catalysis A: Chemical 381 (2014) 1– 8.

[17] Y. Zheng, F. Duan, M.Q. Chen, Y. Xie, Synthetic $Bi_2O_2CO_3$ nanostructures: novel photocatalyst with controlled special surface exposed, *J. Mol. Catal. A: Chem.* 317 (2010) 34–40.

[18] E.J. Li, K. Xia, S.F. Yin, W.L. Dai, S.L. Luo, C.T. Au, Preparation, characterization and photocatalytic activity of Bi_2O_3–MgO composites, *Mater. Chem. Phys.* 125 (2010) 236–241.

[19] F. Krok, I. Abrahams , A. Zadrozna, M. Małys, W. Bogusz, J.A.G. Nelstrop, A.J. Bush, Electrical conductivity and structure correlation in BIMNVOX, *Solid State Ionics* 119 (1999) 139–144.

[20] N.A.S. Al–Areqi, S. Beg, Phase transition changes in $Bi_4Ce_xV_{2-x}O_{11-(x/2)-\delta}$ system, *Mater. Chem. Phys.* 115 (2009) 5–8.

[21] R.D. Shannon and C.T. Prewitt, Effective ionic radii in oxides and fluorides, *Acta Crystallogr. B* 25 (1969) 925–946.

[22] E. Pernot, M. Anne, M. Bacmann, P. Strobe1, J. Fouletier, R.N. Vannier, G. Mairesse, F. Abraham, G. Nowogrocki, Structure and conductivity of Cu and Ni–substituted $Bi_2V_2O_{1\ 1}$ compounds, *Solid State Ionics* 70–71 (1994) 259–263.

[23] M. Alga, A. Ammar, R. Essalim, B. Tanouti, A. Outzourhit, F. Mauvy, R. Decourt, Study on structural, thermal, sintering and conductivity of Cu–Co doubly substituted $Bi_4V_2O_{11}$, *Ionics* 11 (2005)81–86.

[24] A. Watanabe , K. Das, Time–dependent degradation due to the gradual phase change in BICUVOX and BICOVOX oxide–ion conductors at temperatures below about 500°C, *J. Solid State Chem.* 163 (2002) 224–230.

[25] W. Wrobel, I. Abrahams, F. Krok, A. Kozanecka, M. Malys, W. Bogusz, J.R. Dygas, Phase stabilization and electrical characterisation in the pseudo–binary system $Bi_2ZrO_{5.}$–$Bi_2VO_{5.5–\delta}$, *Solid State Ionics* 175 (2004) 425–429.

[26] X. Yang, F. Ma, K. Li, Y. Guo, J. Hu, W. Li, M. Huo, Y. Guo, Mixed phase titania nanocomposite codoped with metallic silver and vanadium oxide: New efficient photocatalyst for dye degradation, *J. Hazard. Mater.* 175 (2010) 429–438.

[27] I. Abrahams, F. Krok, Defect chemistry in the BIMEVOXes, *J.Mater.Chem.*12(2002)3351–3362.

[28] S. Beg, A. Al–Alas, N.A.S. Al–Areqi, Layered Aurivillius compound: Synthesis, characterization and electrical properties, *J. Alloys and Compds* 504 (2010) 413–419.

[29] N.S.A. Al–Areqi, S. Beg, A. Al–Alas, Study on phase stability and oxide ion conductivity in the BIAGVOX system, *J. Phys. Chem. Solids* 73(2012)730–734.

[30] H. R. Pouretedal, M. H. Keshavarz, Synthesis and characterization of $Zn_{1–X}Cu_XS$ and $Zn_{1–X}Ni_XS$ nanoparticles and their applications as photocatalyst in Congo red degradation, *J Alloys Compds* 501 (2010) 130–135.

[31] C. Bauer, P. Jacques, A. Kalt, Photooxidation of an azo dye induced by visible light incident on the surface of TiO_2, J. Photochem. Photobiol. A–Chem. 140 (2001) 87–92.

[32] I.K. Konstantinou, T.A. Albanis, TiO_2–assisted photocatalytic degradation of azo dyes in aqueous solution: kinetic and mechanistic investigations: a review, *Appl. Catal. B–Environ.* 49 (2004) 1–14.

[33] J. S. Im, B. C. Bai, S. J. In, Y. S. Lee, Improved photodegradation properties and kinetic models of a solar–light–responsive photocatalyst when incorporated into electrospun hydrogel fibers, *J. Colloid Interface Sci.* 346 (2010) 216–221.